UCRL - 75883
PREPRINT
Conf-741079--13

LAWRENCE LIVERMORE LABORATORY
University of California/Livermore, California

HEATING AND CONDUCTION IN LASER-PRODUCED PLASMAS

Henry D. Shay, George B. Zimmerman
and John H. Nuckolls

October 28, 1974

This paper was prepared for submission to the 16th Annual Meeting of the Division of Plasma of the American Physics Society, October 28-31, 1974 Albuquerque, N. M.

HEATING AND CONDUCTION IN LASER-PRODUCED PLASMAS *

Henry D. Shay, George B. Zimmerman, John H. Nuckolls

A series of experiments conducted by G. McCall[1] of LASL provides important clues concerning the electron distributions heated in the absorption of intense ($\lesssim 10^{16}$ W/cm^2) laser radiation and the thermal transport of energy. Presented here is a tentative interpretation of these experiments obtained from LASNEX[2] calculations.

SLIDE 1

G. McCall conducted these experiments with a Nd:glass laser producing pulses of 10-16 J with a FWHM of 30 ps; these pulses had an 800 ps precursor with a power roughly 10^5 smaller than the peak power. The focal spot had a FWHM of roughly 120 μm. The focal spot diameter was measured by a variety of methods, the most definitive of which was the direct observation of the diameter of the plasma plane at the peak of the pulse.

Both thick ($\sim$ 150 μm) and thin ($d \ll 1$ μm) CH and CH_2 targets were employed in these studies. In this study, only the more energetic shots are considered: $\approx$ 10 J and $\approx$ 16 J, respectively. The x-ray spectrum measured in the thick target experiments spans the range, $5 \leq h\nu \leq 50$ keV, and, thus, provides information on the shape of suprathermal electron distribution. In the thin target experiments, there are two additional kinds of measurements: the fraction of light transmitted through the plasma (a measure of the length of time required for the entire foil to go underdense)

*Research performed under the auspices of the U. S. Atomic Energy Commission.

and ion velocities in the blow-off on either side of target. These data are quite sensitive to the rate of thermal conduction, both into the dense foil and along its surface.

In the accounting of laser energy, McCall reports that about 84% of the energy from the laser is actually incident upon the target; the remaining 16% is lost in the optics. Of the 84% incident upon the plastic foil, 50% is either transmitted or absorbed in a small spot. Since the fraction reflected is small (< 10%), roughly 50% of the incident energy has apparently disappeared. The amount absorbed was measured both by the observation of the blast wave velocity when the irradiation was conducted in a low pressure environment and by the size of a blast crater in a slab target. Consequently, the estimates of absorbed energy do not include any absorption distributed over very large radii and, hence, at very low intensity. The fraction of energy transmitted through the foil is a function of the foil thickness,varying roughly as exp (-d/500 Å).

Virtually all the ion flow-off is funneled into narrow velocity cones centered on the front and rear normals to target foil--the pulses were so short that the hydrodynamic expansion was nearly one dimensional. The current trace of an ion probe for representative shots may be characterized by a mean time of flight. For foils 1800 Å thick the ratio of the fore and aft mean ion velocities is about 4; for 300 Å, about 1. On many shots, the current pulse is divided into two well-defined peaks. These may be tentatively identified as the arrival of H^+ and C^{6+} ions with both species accelerated through the same electrostatic plasma potential.

SLIDE 2

A representative front ion current trace (for a low energy shot, $E_0 \simeq 3.7$ J) illustrates the separation of the ion current pulse into two peaks. Since LASNEX is a Lagrangian hydrodynamic code which permits neither charge separation (by the requirements of $\vec{J} = 0$) nor distinct velocities for different ionic species, the study cannot reproduce these details and considers comparison only with the mean ion velocity, <v>, shown on this slide. This velocity is here defined merely as the mean of two velocities v and v'. Since significant kinetic energy may be present in the long tail of ions arriving at much later times, this mean, <v>, may actually be a slight overestimate.

SLIDE 3

McCall's thin foils have the great advantage that a single parameter, an effective spot radius, r_{eff}, suffices to specify the total mass heated, M. Moreover, within the context of a simple model, which assumes merely one dimensional blow-off and well-defined fore and aft mean blow-off velocities, the effective spot size may be determined solely from fore-aft ion velocities, without any integration over time and space to determine the number of participating ions. Suppose, for example, that the heated area is much larger than the measured laser spot size and that some mass M_F (M_B) is blown forward (backward) with velocity v_F (v_B). The laws of the conservation of mass, momentum, and energy then imply a simple relationship between E_A/M and the two velocities, v_F and v_B.

The measurements conducted with, for example, the 1800 Å thick foils imply that the effective spot diameter is $\simeq$ 550 μm, that is, that the laser energy is distributed over a target mass more than 20 times greater than expected on

the basis of the laser spot diameter. This analysis may also be conducted with two separate velocities for H^+ and C^{6+} ion species with identical results. The fact that <v> is an overestimate implies that this estimate of reference is a lower bound. LASNEX simulations also confirm that ion velocity measurements imply a huge effective spot size. One may postulate a variety of mechanisms causing this effect: lateral conduction, refraction, ... and this investigation has examined the plausible causes.

SLIDE 4

The crucial approximations used in the LASNEX simulations are electron distributions associated with resonance absorption and inhibited electron thermal conduction. Kruer, et al.[3], have found that at these laser intensities resonance absorption is the dominant process, not inverse bremsstrahlung nor a parametric instability. Their calculations indicate that, when the evolution of density gradient is computed self-consistently, resonance absorption is efficient over a wide range of angles and the distribution of heated electron is $\exp(-v^2/\alpha v_{th}^2)$, where $6 \leq \alpha \leq 12$. LASNEX computes the transport of these electron by means of a multi-group, flux-limited diffusion approximation.

LASNEX calculations in which Spitzer estimates are used for diffusion coefficients, cannot reproduce the ion TOF or the transmitted light data. The data are consistent with inhibited thermal conduction. Several possible mechanisms are noted on this slide. For those conditions in which the ion temperature is much less than the electron temperature, the flow of electrons

through the ions is subject to a two stream stability. Fried and Gould[4] have calculated the region of stability as a function of V_{DRIFT}/V_e and θ_e/θ_i, as shown on this slide. Since the growth rate on this instability is large, that is, roughly comparable to the ion plasma frequency, one may anticipate that the instability would rapidly reduce the drift velocity to the critical drift velocity. Accordingly, the approximation for this process used in LASNEX is the reduction of the flux limits of each electron group by the local, instantaneous ratio of V_{CRIT}/V_e where v_e and θ_e are determined from the thermal electron group. In this treatment, then, the drift velocities of both the fast electrons and the cold counter-streaming electrons are diminished. Since the current continuity equation demands that the suprathermal flow be balanced by a counter flow, any impedance to the counter flow inhibits as well the suprathermal flow. The suprathermal flow is also diminished, of course, by the reduction of its own flux-limiters. Another possible, though crude, representation of the two-stream instability would be to reduce globally all electron flux-limiters by some typical factor, 30 for example. Both prescriptions have been used alternatively in these calculations to assess anomalous conduction.

Another mechanism possibly responsible for inhibiting thermal conduction is the generation of strong magnetic fields. LASNEX calculates the magnetic fields arising from thermo-electric sources, $\nabla\theta_e \times \nabla n_e$, and the subsequent reduction of thermal conductivity, by the Braginskii or the Bohm approximation. For a fairly smooth variation in laser intensity across the focal spot, these fields assume a toroidal configuration wrapped about the axis of revolution.

Consequently, such magnetic fields approach zero at the center of the laser spot, and thus, while effective in impeding lateral conduction, cannot drastically reduce conduction into the target.

Recent plasma simulation conducted by Kruer, et al.[5], suggest that very intense laser radiation obliquely incident upon a target generates large magnetic fields which are laminar within the focal spot. This is an alternate mechanism for the inhibition of thermal conduction.

SLIDE 5

Here are summarized the results of 1-D LASNEX calculation for two thin foil experiments. Resonance absorption with $\alpha = 12$ and the anomalous conductivity prescription based on Fried and Gould's work are assumed. Without the assumption of anomalous conductive, the computed E_T/E_A for 300 Å is too large and $\langle v_F \rangle / \langle v_B \rangle$ is roughly 1, instead of exhibiting the distinct fore-aft asymmetry. These results demonstrate that the data imply an inhibited thermal conduction.

SLIDE 6

The x-ray data is the most sensitive to the electron distribution. The three spectra predicted with the assumption of anomalous conductivity and with $\alpha = 1$, 6, and 12 illustrate that the $\alpha = 6$ distribution results in the best agreement between theory and experiment.

The mean velocity determines the effective spot size; the fore-aft velocity ratio and the ratio of transmitted and absorbed laser radiation indicates the presence of inhibited conduction; the shape of the x-ray spectrum implies that α is roughly six. This interpretation hinges, of

course, upon an adequate understanding of the large effective spot size. A series of 2-D LASNEX calculations have isolated the most plausible choices.

SLIDE 7

One possibility is that the laser light is so greatly refracted in the underdense plasma that a much larger spot is actually illuminated. This speculation is disproven by several LASNEX calculations utilizing the recently implemented geometrical optics ray trace[6], as illustrated in this snap shot taken at the peak of the calculated laser pulse. Because of the short pulse length, the density gradient at the critical density, marked in dashed lines, is very steep and the laser rays have scarcely any curvature in traversing the underdense plasma. In these experiments, in contrast to experiments conducted with longer laser pulses, one may not reasonably expect that refraction play an important role.

SLIDE 8

2-D LASNEX calculations have demonstrated that a very small amount of rarified plasma blow-off serves as a very low impedance conduction path and greatly enhances, thereby, lateral conduction. This slide depicts a plasma in an experiment conducted with a 1800 Å foil, viewed at the peak of the laser pulse. The dashed lines represent isodensity contours; the solid lines, electron isotherms. The laser intensity profile used in this calculation is a Gaussian with a FWHM of 120 μm, the observed beam spot size, but to a radius of 100 μm; at larger radii, the intensity is constant,

about one hundredth of the peak intensity, out to a radius of 300 μm. The energy content in this low intensity tail corresponds to one-half of the measured E_D, the disappeared energy. This laser beam profile is, thus plausible.

The peak electron temperature at this time is about 950 eV. The 700 eV isotherm extends out to a radius of 300 μm -- this temperature distribution is graphical evidence of the enlargement of the effective spot size. One should note also that an interferometric picture which probes to electron densities of 10^{18} - 10^{19} cc^{-1} ($\approx 3 \times 10^{-5}$ - 3×10^{-6} g/cc) would indicate a plume less than 200 μm in diameter and relatively blow-off at larger radii. These density profiles are, therefore, consistent with McCall's observations.

Any mechanism which would creat a low density plasma at large radii (eg., heating by uv radiation or laser precursor) results in a similar enlargement of the target spot.

In this calculation the electrons responsible for thermal transport are energetic, $1/2\ m\ v_e^2 \gtrsim 20$ keV. The mean free paths of such electrons in solid density material are comparable to the dimensions of the effective spot size. The enhancement of lateral conduction arises instead from the reduction of the mean free path of the cold return current: for example, the mean free path of 1 keV electron in a 1 keV C^H plasma is $\sim .05$ μm at 1 g/cc, but ~ 50 μm at 10^{-4} g/cc. In a similar calculation, thermo-electrical induced magnetic has peak of 300 kG at $r \simeq 150$ μm. At these magnetic inductions, the gyro-magnetic radius of the counter-streaming electrons is just a

few microns. The computations indicate that the predicted x-ray spectrum diverges radically from the measured when the Braginiskii approximation is used, but that the agreement is satisfactory when Bohm diffusion is used.

These 2-D LASNEX calculations predict that the ion blow-off is funnelled in a narrow cone, as is observed. The ion TOF and transmitted light predictions corraborate qualitatively with those predicted in the 1-D calculation using 600 μm effective spot sizes. While the 2-D calculations do reproduce McCall's data, this agreement is not wholly satisfactory since the Fried and Gould prescription was used in the thin foil calculations, but the constant factor reduction of the electron flux limiters (.03) was required in the thick slab calculations.

There remains the possibility that laminar magnetic fields, ponderomatively induced, exist in the focal spot. Kruer, et al.[5], have calculated that megagauss fields would be generated near the critical density at these intensity for laser beams at fairly large angles ($\sim 30^{o}$) to the normal. Such magnetic fields could suffice to inhibited thermal conduction into the target. These comments are now, of course, speculative and detailed predictions await more calculations.

In conclusion, in this interpretation, the data imply:

1) The effective spot size is much larger than the laser spot. Lateral conduction along the surface of the foil is responsible for this effect.
2) Thermal conduction is inhibited by ion-electron turbulance or, perhaps, by sheet magnetic fields.
3) Suprathermal electrons are heated in distribution $f(v) \alpha \exp(-v^2/6v_{th}^2)$.
4) Bohm diffusion is the appropriate approximation for transverse thermal transport.

REFERENCES

1. G. McCall, private communication.

2. G. B. Zimmerman, Numerical Simulation of the High Density Approach to Laser-Fusion, Lawrence Livermore Laboratory, Rept.,UCRL-74811 (1973).

3. K. G. Estabrook, E. J. Valeo, and W. L. Kruer, Two-Dimensional Relativistic Simulations of Resonance Absorption, Preprint, UCRL-75613 (1974).

4. Fried and Gould, Phys. of Fluids, 4, 139 (1961).

5. W. L. Kruer, Bull. Am. Phys. Soc., 19, 899 (1974).

6. D. S. Bailey, ibid, 868; Yu-Li Pan and H. D. Shay, ibid.

Experiments using Nd:Glass pulse: 30 ps; 10-16 J; diameter $\simeq$ 120 μm

1). Thick (150 μm) CH target (E_o = 10 J)

x-ray spectrum 5-50 keV

2). Thin ($<<$ 1 μm) CH target (E_o = 16 J)

Light transmission
- $E_T/E_o = .84 \times .50 \exp(-d/500\ \text{Å})$
- $E_A/E_o = .84 \times .50\ (1 - \exp[-d/500\ \text{Å}])$
- $E_D/E_o = .84 \times .50$

Ion TOF
- a). d = 1800 Å
  - front
    - $v = 1.5 \times 10^8$ cm/sec (H^+)
    - $v' = 9.6 \times 10^7$ cm/sec (C^{6+})
  - back
    - $v = 3.4 \times 10^7$ cm/sec (H^+)
    - $v' = 2.5 \times 10^7$ cm/sec (C^{6+})
  - $v_F/v_B \approx 4$
- b). d = 300 Å
  - $v_F/v_B \approx 1$

FIGURE 1

ION CURRENT – TIME OF FLIGHT

Forward direction

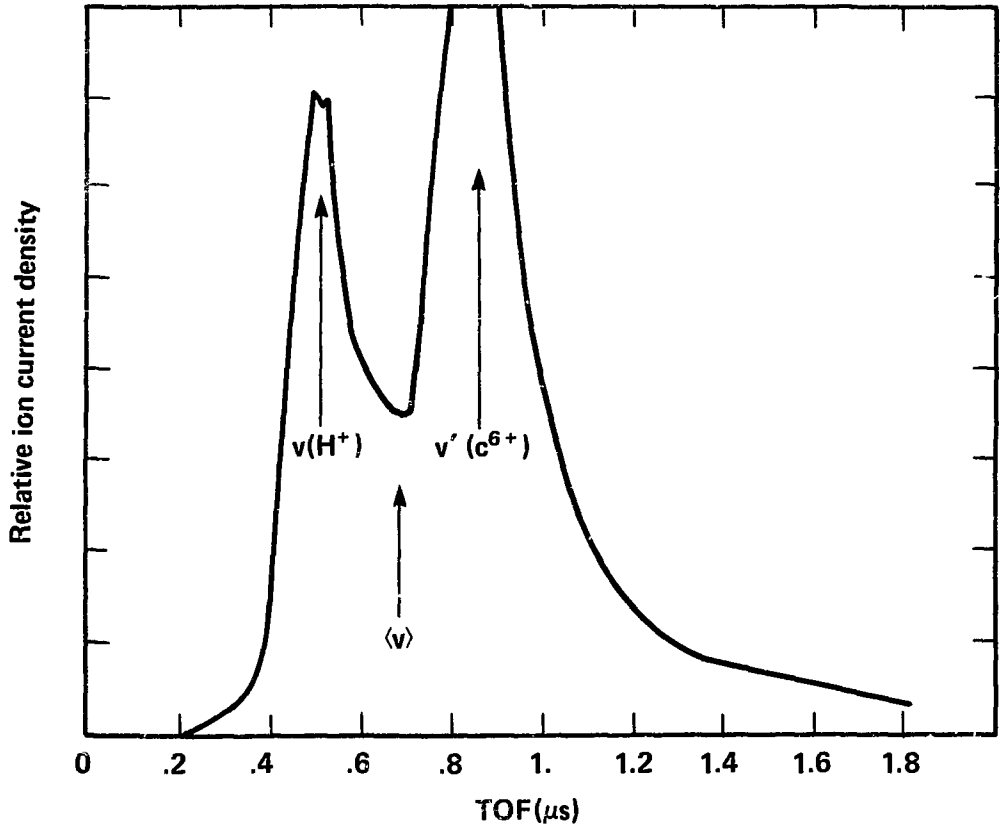

FIGURE 2

EFFECTIVE SPOT SIZE

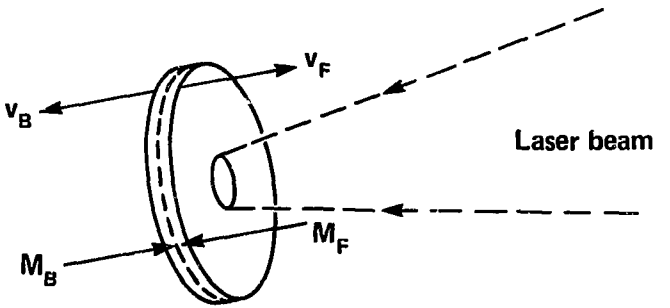

FIGURE 3

Conservation laws:

$$M = M_F + M_B$$

$$O = M_F\, v_F - M_B\, v_B$$

$$E_A = \tfrac{1}{2} M_F v_F^2 + \tfrac{1}{2} M_B\, v_B^2$$

$$\Rightarrow\ E_A/M = \tfrac{1}{2}\left[\frac{v_B\, v_F^2}{v_B + v_F} + \frac{v_F\, v_B^2}{v_B + v_F}\right]$$

$\Rightarrow$ for 1800 Å foil experiments,

$$E_A/M \simeq 1.7 \times 10^{15}\ (\text{cm/sec})^2$$

$$\Rightarrow\ 2\, r_{eff} \gtrsim 550\ \mu\text{m}$$

LASNEX MODEL

* Resonance absorption with self-consistently steepened density gradient:

$f_e(v) \propto \exp(-v^2/\alpha v_{th}^2)$, $6 \leqslant \alpha \leqslant 12$

* Reduced thermal conductivity:
  - Electron-ion turbulence

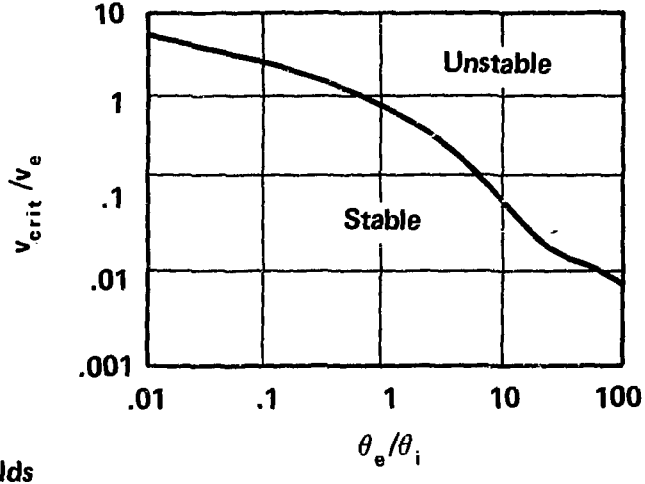

  - *Magnetic fields*
    - Thermal source – toroidal

$$\frac{\partial \vec{B}}{\partial t} \propto \nabla\theta_e \times \nabla n_e$$

    - Ponderomotive source – laminar

FIGURE 4

1-D LASNEX CALCULATIONS: ION TOF AND TRANSMITTED LIGHT

Spot diameter = 600 μm ; α = 12

	E_T/E_A		$\langle v_F \rangle / \langle v_B \rangle$		$\langle v_F \rangle$, cm/sec	
d(Å)	Exp.	Calc.	Exp.	Calc.	Exp.	Calc.
300	1.2	1.0	≈ 1	.7	—	10^8
1800	0.	0.	≈ 4	1.8	1.2×10^8	8.7×10^7

FIGURE 5

X-RAY SPECTRA FOR VARIOUS ELECTRON DISTRIBUTIONS

1-D calculations:
600μm diameter
with anomalous
conductivity

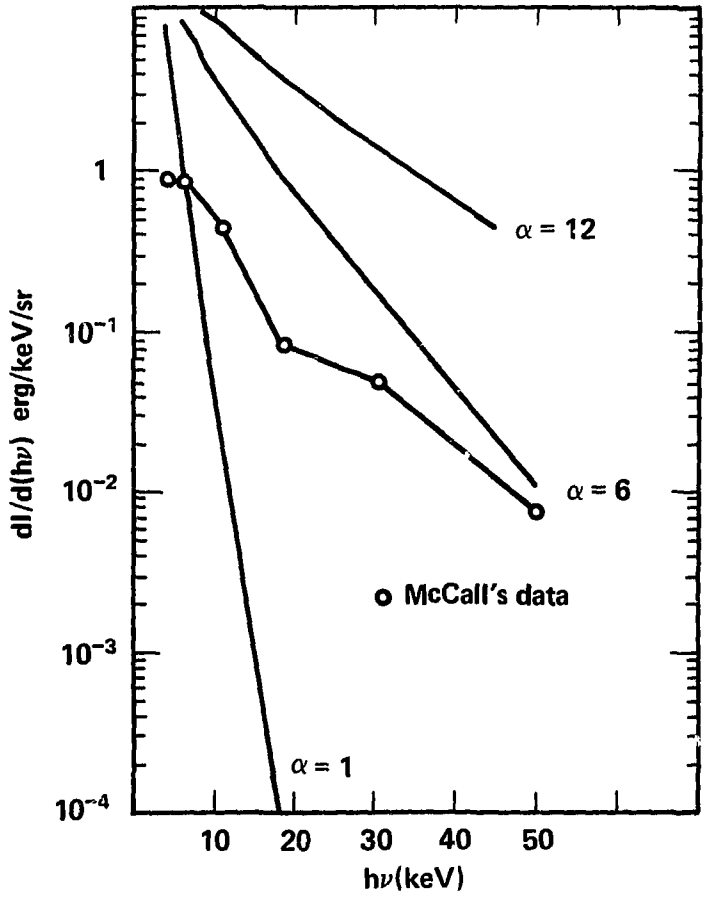

FIGURE 6

REFRACTION IN UNDER-DENSE PLASMA

t = peak of pulse

1800 Å

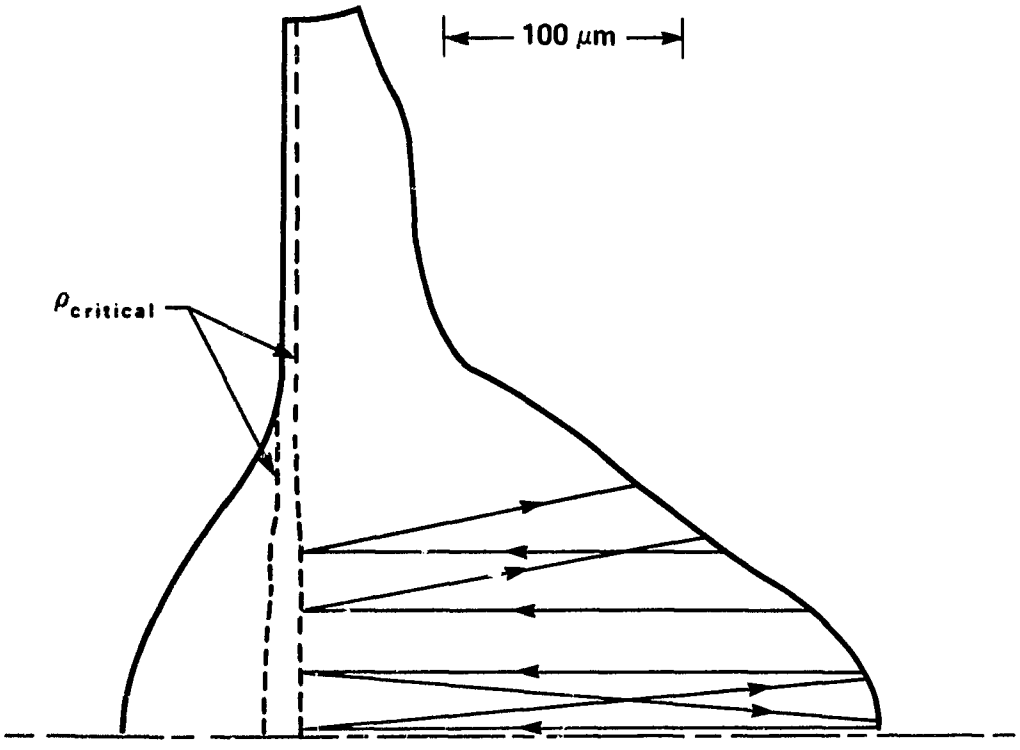

FIGURE 7

ENLARGEMENT OF SPOT

Lateral thermal conduction in rarified region
t = peak of pulse
1800 Å

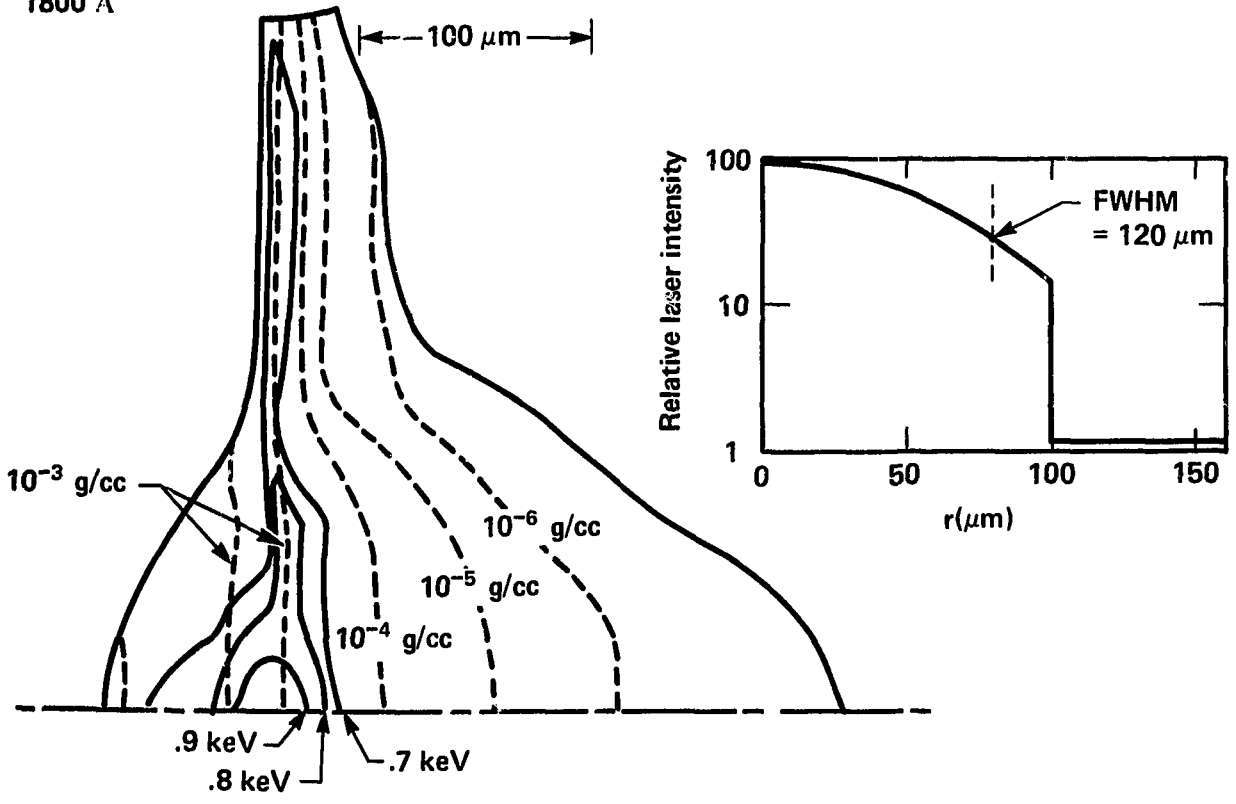

FIGURE 8